CRITICAL PLANE APPROACH IN STAGE I AND STAGE II OF FATIGUE UNDER MULTIAXIAL LOADING

A. Karolczuk, E. Macha

Opole University of Technology, Faculty of Mechanical Engineering, ul. Mikolajczyka 5, 45-271 Opole, Poland, karol@po.opole.pl, emac@po.opole.pl

Abstract. This paper deals with the estimation problem of the critical plane orientation in multiaxial fatigue failure criteria. Experimental results from multiaxial proportional, non-proportional cyclic loading and variable-amplitude bending and torsion were used to determine the macroscopic fracture plane orientations and the fatigue lives. It was concluded that more important than macroscopic fracture plane orientation is the evolution (Stage I, Stage II) of fracture planes and an appropriate choice of the fatigue failure criterion for the fatigue life estimation.

Introduction

Numerous multiaxial fatigue failure criteria based on the critical plane approach have been proposed [1-4]. This approach assumes that some stress or/and strain components acting on the critical plane are responsible for the fatigue failure of the material. It is based upon the experimental observation that fatigue cracks initiate and grow on the certain material planes. The critical plane criteria define different functions that combine the shear and normal stress or/and strain components on a plane into one equivalent parameter. It is commonly accepted that depends on the test conditions (loading level, temperature, material type, state of stress, ect.) material generally forms one of the two types of cracks - shear cracks or tensile cracks. The shear cracks are formed on the maximum shear stress plane and Forsyth [5] called this process as Stage I. The tensile cracks are formed in Stage II that is predominated by the maximum normal stress component. The equivalent damage parameter is usually compared to the uniaxial shear or tensile damage parameter obtained by the experimental tests under torsion or push-pull loading (S-N curves). However, it is also accepted that either under multiaxial and uniaxial fatigue tests the cracks may initiate and propagate on different planes – contradictory to the one critical plane orientation. To solve this problem, a wide range of multiaxial fatigue failure criteria were proposed only for materials and test conditions for which one of the two stages (I or II) dominates in the total fatigue life. There are two aspects in the critical plane approach that should be discussed: (i) Should the critical plane orientation be determined by the maximum shear or normal stress/strain component or rather by the plane with the highest damage degree estimated using the equivalent damage parameter? (ii) Should the critical plane orientation coincide with the fatigue fracture plane position at the microscale or macroscale? Based on the experimental results analysed in this paper, some comments will be drawn to the mentioned aspects.

The Findley Criterion

Findley [1] proposed a linear combination of the maximum normal stress $\sigma_{n,\max}$ and the shear stress amplitude $\tau_{ns,a}$ on the critical plane for a given number of cycles to failure N_f

$$\tau_{ns,a} + k\sigma_{n,\max} = f \, , \tag{1}$$

where f and k are the material coefficients. The critical plane orientation coincides with the plane orientation where the maximum value of this linear combination occurs. Findley did not define a mathematical formula for the material coefficient f. Some researchers [6, 7] assume that it can be determined from the shear-mode cracking

$$\tau_{ns,a} + k\sigma_{n,\max} = \tau_{af}\left(\frac{N_\tau}{N_f}\right)^{1/m_\tau} , \tag{2}$$

where τ_{af}, m_τ are the fatigue limit and the exponent of the S-N curve for fully reversed (R=-1) torsion loading, respectively; N_f is the considered number of cycles to failure; N_τ is the number of cycles corresponding to the fatigue limit τ_{af} for fully reversed torsion loading.

The Findley criterion and other are based on the cyclic properties of fatigue loading for which the amplitude of the shear stress $\tau_{ns}(t)$ can be found. The problem appears under random loading. Nevertheless, it is possible to adapt the Findley and other criteria to random loading. For the Findley criterion, the equivalent stress course is as follows

$$\tau_{eq}(t) = \tau_{ns}(t) + k\sigma_n(t). \tag{3}$$

The equivalent shear stress history $\tau_{eq}(t)$ at observation time T is then used as the cyclic counting variable. In this case, the range of amplitudes could be divided into the finite numbers of stress levels. For each *i-th* stress level $\tau_{eq,a}^{(i)}$, damage degree is computed by the general equation as follows

$$D^{(i)} = \begin{cases} \dfrac{n^{(i)}}{N_f^{(i)}} & for \quad F_{eq,a}^{(i)} \geq aF_{af} \\ 0 & for \quad F_{eq,a}^{(i)} < aF_{af} \end{cases}, \tag{4}$$

where F is the generalised fatigue damage parameter (for the Findley criterion: $F=\tau$), $n^{(i)}$ is the number of cycles assigned into the *i-th* stress level, a is a coefficient allowing to include amplitudes below F_{af} in the damage accumulation, $N_f^{(i)}$ is a computed number of cycles to failure for the *i-th* stress level (e.g. by Eq. (2)). It is assumed that $a = 0.5$ is sufficient, for lower value, the damage degree is too small to be taken into account.

The Matake Criterion

Matake [2] introduced a linear combination of the shear and normal stresses on the critical plane, similar to the Findley proposal

$$\tau_{ns,a} + k\sigma_{n,a} = \tau_{af}\left(\frac{N_\tau}{N_f}\right)^{1/m_\tau}, \tag{5}$$

where $\sigma_{n,a}$ is the normal stress amplitude on the critical plane. However, the critical plane orientation coincides with the plane of the maximum shear stress amplitude. For such orientation of the critical plane, it is possible to determine the material coefficient $k = 2\tau_{af}/\sigma_{af} - 1$.

Under random loading, the equivalent shear stress history has the same mathematical form as Eq. (3). However, for the Matake criterion the maximum shear stress range $\Delta\tau_{ns}$ determines the critical plane orientation

$$(\vec{n}, \vec{s}) : \Delta\tau_{ns} = \max_{0<t<T}\{\tau_{ns}(t)\} - \min_{0<t<T}\{\tau_{ns}(t)\}, \tag{6}$$

where T is the time of observation. Damage degree $D^{(i)}$ is computed on the critical plane for each *i-th* stress level according to the general Eq. (4), where $F=\tau$.

The Maximum Normal Stress Criterion On The Critical Plane

This failure criterion comes from the static hypothesis of material strength. According to this criterion, the maximum normal stress range is responsible for the fatigue of materials. For the cyclic loading it leads to the following equation

$$\sigma_{n,a} = \sigma_{af}\left(\frac{N_\sigma}{N_f}\right)^{1/m_\sigma}, \tag{7}$$

where m_σ is the exponent of the S-N curve for fully reversed (R=-1) push-pull loading; N_σ is the number of cycles corresponding to the fatigue limit σ_{af}.

For random loading the equivalent stress history is as follows

$$\sigma_{eq}(t) = \sigma_n(t). \tag{8}$$

Damage degree $D^{(i)}$ is computed on the critical plane for each *i-th* stress level according to the general Eq. (4), where $F = \sigma$.

Damage Degree Accumulation And Fatigue Life Calculation

For the variable-amplitude loading, a linear damage Sorensen-Kogayev accumulation hypothesis [8] was applied

$$D = \frac{1}{p}\sum_{i=1}^{j} D^{(i)} \; , \quad p = \frac{\sum_{i=1}^{j} F_{eq,a}^{(i)} f^{(i)} - a F_{af}}{F_{eq,a}^{\max} - a F_{af}} \; , \quad f^{(i)} = \frac{n^{(i)}}{\sum_{i=1}^{j} n^{(i)}} \tag{9}$$

where $D^{(i)}$ is the damage degree computed according to the general Eq. (4), p is the hypothesis coefficient, j is the total number of loading levels (we assume $j = 64$), $f^{(i)}$ is the frequency of the *i-th* loading level, $F_{eq,a}^{\max}$ is the maximum amplitude of the generalised fatigue damage parameter ($F = \tau, \sigma$). Accumulated damage degree D at the observation time T is used to estimate the fatigue life according to the following expression

$$T_{cal} = \frac{T}{D(T)} \, , \tag{10}$$

In the case of the cyclic loading, the number of cycles to failure N_f is computed directly from Eqs (2), (5), (7) and then recalculated to $T_{cal} = N_f/f$, where f is the frequency of the cyclic loading.

Fatigue Tests

Detailed information about the experimental setup could be found in [9]. Fatigue tests were performed on the round full cross-section specimen made of 18G2A steel under constant- and variable-amplitude combined bending and torsion moment histories measurement (bending: $M_b(t)$, torsion: $M_t(t)$). Some mechanical properties of the 18G2A steel are shown in Tab. 1.

Table 1. Mechanical properties of the 18G2A steel

Property	Value
Quasi-static yield stress (σ_y, MPa) and ultimate strength (σ_u, MPa), respectively	357, 535
Young's modulus (E, GPa) and Poisson's ratio (ν)	210, 0.30
Fatigue limit for fully reversed torsion loading, τ_{af}, MPa (*)	142.5
Exponent of the S-N curve for fully reversed torsion loading, m_τ (*)	12.3
Number of cycles corresponding to the fatigue limit τ_{af} for fully reversed torsion loading, N_τ, cycles	$1.98 \cdot 10^6$
Fatigue limit for fully reversed push-pull loading, σ_{af}, MPa	204
Exponent of the S-N curve for fully reversed push-pull loading, m_σ,	8.2
Number of cycles corresponding to the fatigue limit σ_{af} for fully reversed push-pull loading, N_σ, cycles	$1.24 \cdot 10^6$

(*) – value recalculated from the torsion S-N curve performed on the full round cross-section specimen using the algorithm presented in the next paragraph.

For the constant-amplitude sinusoidal proportional and non-proportional (phase shift $\delta = \pi/2$) loading, the tests were carried out with a frequency $f = 20$ Hz under different ratios of the torsion and bending moments $\lambda_M = M_{t,max}/M_{b,max}$. For the variable-amplitude loading, the specimens were subjected to bending or torsion with a normal probability distribution and a narrow frequency band. The fatigue life and the macroscopic fatigue fracture plane orientation was determined for each specimen. The experimental results are presented in Tab. 2, where $\hat{\alpha}_{exp}$ is the averaged value of experimental angles α_{exp}, $<\hat{\alpha}_{\min} \div \hat{\alpha}_{\max}>$ is the confidence interval (assuming a normal distribution of the α_{exp}) which contains 50% of the probability and α_{exp} is the angle between unit-normal vector $\vec{n}$ to crack plane and the specimen axis **z**.

Two fatigue crack behaviours were observed: (i) one general crack orientation at the macroscale was detected under all the investigated constant-amplitude loadings and under the variable-amplitude bending; (ii) two crack orientations were observed for the specimens subjected to variable-amplitude torsion. The first orientation with a crack length of around 0.15-0.3 mm is parallel to the specimen axis. The other orientation comes from branching of the primary crack, and these branching directions are inclined to the specimen axis by around 45° (load case no 7 in Tab. 2).

Table 2. Experimental data

No	δ	$M_{b,max}$	λ_M	$\hat{\alpha}_{exp}$	$<\hat{\alpha}_{min} \div \hat{\alpha}_{max}>$
	rad	Nm	-	[^{o}]	[^{o}]
Constant-amplitude loading					
1	0	8.0; 10.0; 10.3	0.68	18.1	17.1 ÷ 19.0
2	0	6.4; 7.4; 8.2; 9.8	0.96	21.9	20.0 ÷ 23.8
3	0	5.3; 6.2; 7.2;	1.44	26.5	23.8 ÷ 29.2
4	$\pi/2$	8.9; 9.2; 9.6; 10.3	0.68	12.3	9.1 ÷ 15.5
5	$\pi/2$	8.3	0.98	8.4	7.3 ÷ 9.5
6	$\pi/2$	6.4; 7.2	1.42	10.2	6.4 ÷ 13.9
Variable-amplitude loading					
7	-	18.4	∞	43.6/86.3	42.2÷45.0/82.3 ÷ 90.2
8	-	16.3	0	1.5	0.8÷2.2

Stress And Strain Computations

Stress and strain histories in an arbitrary point (x, y) of the specimen cross-section were computed from bending and torsion moments $M_b(t)$, $M_t(t)$ considering the plastic strains. Plasticity was included in the computation since the cyclic properties (K', n') of the 18G2A steel reveal the appearance of the plastic strains even under low stress level ($\varepsilon_a^p = 0.65\%$ for $\sigma_{af} = 204$ MPa). The Chu [10] plasticity model of material behaviour was applied to determine the strain-stress relation and the influence of loading history on the strain state for each point of the specimen cross-section. For every increment of bending $\Delta M_b(t)$ and torsion $\Delta M_t(t)$ moments the following quasi-static equilibrium equations were solved by the trust-region method

$$\int_A \Delta\sigma_{zz}(x,y,t)y dA - \Delta M_b(t) = 0, \quad \int_A \Delta\tau_{z\phi}(\rho,t)\rho dA - \Delta M_t(t) = 0, \tag{11}$$

where the increment Δ is defined as $\Delta\sigma_{zz}(x, y, t) = \sigma_{zz}(x, y, t+\Delta t) - \sigma_{zz}(x, y, t)$; $\Delta\sigma_{zz}$ is the normal stress increment for the finite element with the origin in the plane (x, y); $\Delta\tau_{z\varphi}(t, \rho)$ is the shear stress increment for the finite element with the origin determined by the radius $\rho = \sqrt{x^2 + y^2}$; dA is the area of the finite element. Detailed information about the stress and strain computations are presented in [11].

Evaluation And Discussion

The following error parameters were analised to compare the experimental macroscopic fracture plane orientation with the critical plane orientation

$$E_\alpha^{(i)} = \left| \hat{\alpha}_{exp}^{(i)} - \alpha_{cal}^{(i)} \right|, \quad E_{\alpha,m} = \frac{1}{N}\sum_{i=1}^{N} E_\alpha^{(i)}, \tag{12}$$

where N is the number of load cases ($N = 8$), analysed α range ($\alpha \in$ <-90°, 90°>, $\Delta\alpha$=0.1^o). Absolute difference $E_\alpha^{(i)}$ and the mean value $E_{\alpha,m}$ computed according to the analysed criteria are presented in Table 3. Bold face characters are used for error parameters smaller than 5°.

Table 3. Error parameters: $E_\alpha^{(i)}$, $E_{\alpha,m}$ computed according to the analysed criteria

No	$\sigma_{zz,max}$ MPa	$\lambda_{\tau\sigma}=$ $\tau_{zx,max}/\sigma_{zz,max}$	Matake, [°] $k=0.4$	Findley, [°], k				max$\{\sigma_n\}$, [°]
				k=0.2	k=0.4	k=0.8	k=1.6	
1	223; 280; 286	0.29	11.8	6.1	**0.9**	7.5	17.2	**3.0**
2	184; 214; 236; 280	0.44	**2.5**	**3.1**	8.4	16.8	17.3	**1.3**
3	156; 182; 212	0.68	8.3	14.0	19.2	25.3	15.7	**0.3**
4	262; 272; 281; 295	0,50	22.2	18.0	14.3	7.5	**0.8**	7.8
5	262	0,62	7.4	58.6	45.4	31.9	20.7	**2.8**
6	250; 278	0,71	10.0	68.9	58.4	42.2	**1.4**	2.9
7	0	∞	**0.9**	5.4	10.9	19.3	29.0	**1.4**
8	280	0	43.5	37.8	32.6	24.2	14.6	**1.5**
		$E_{\alpha,m}$:	13.3	26.5	23.3	21.8	14.6	**2.6**

The macroscopic fracture plane orientation coincides with the maximum shear stress plane (Stage I) only in the case of the pure torsion. In all other cases, the best correlation between macroscopic fracture plane orientation and the critical plane orientation is obtained by the criterion of the maximum normal stress. The Findley criterion was verified for different values of the k coefficient. With increasing the k value the mean error $E_{\alpha,m}$ decreases. However, the smallest mean error for $k = 1.6$ is still larger than the result given by the maximum normal stress plane.

After the critical plane evaluation, the fatigue failure criteria were used to calculate the fatigue life. The following errors parameters were applied for the fatigue life verification:

$$E^{(i)} = \log\frac{T_{cal}^{(i)}}{T_{exp}^{(i)}}, \quad E_m = \frac{1}{N}\sum_{i=1}^{N} E^{(i)}, \quad E_{std} = \sqrt{\frac{1}{N-1}\sum_{i=1}^{N}\left(E^{(i)} - E_m\right)^2}. \quad (13)$$

The mean error parameter E_m reflects the general results conformity. The standard deviation error parameter E_{std} is the superior parameter since it reflects the scatter of the results and therefore gives us the information about the failure criterion ability to correlate the different kind of multiaxial stress states and the equivalent damage parameter. The second-rate parameter E_m depends on the material constants and the stress gradient influence.

Scatter of the results (E_{std}) is very small for the specimens that exhibit one macroscopic fracture plane orientation which coincide with the maximum normal stress plane. The results exposed by the criterion of the maximum shear stress (Table 4) show very large scatter $E_{std} = 0.69$ although the mean error is very small $E_m = 0.05$. The other criteria that combine the shear and normal stress/strain components on the critical plane (Findley, Matake) are not appropriate for the analysed steel (Table 4).
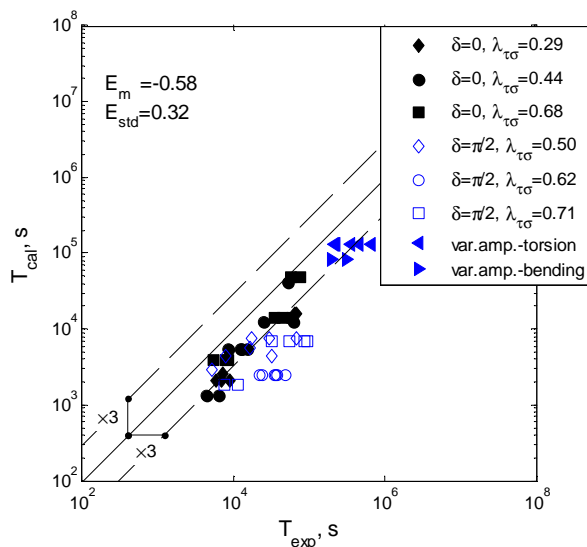

Figure 1. Comparison between the experimental fatigue lives T_{exp} and the calculated fatigue lives T_{cal} for the max$\{\sigma_n, \tau_{ns}\}$ criterion.

From the engineering point of view, the material fracture behaviour is not known before the material fatigue failure and therefore this feature cannot be used as a key in the selection of the fatigue criterion. It was assumed that this selection could be made by the maximum damage degree computed by two simple criteria, i.e. the maximum normal stress criterion (Eq. (7)) and the maximum shear stress criterion (Eq. (3) for k=0). For each specimen, the damage degree on the critical plane is computed by these two criteria (max$\{\sigma_n, \tau_{ns}\}$) and than the

fatigue life T_{cal} is determined by the highest damage degree (Fig.1).

Using this idea, the smallest scatter of the results ($E_{std} = 0.32$) was obtained. It suggests that the fatigue failure under the analysed test conditions is governed only by the maximum normal stresses or by the maximum shear stresses (max$\{\sigma_n, \tau_{ns}\}$).

It should be noticed that the fatigue lifes T_{cal} were estimated using the local approach (only the stress state at one point is analysed) whereas we deal with stress gradients generated by bending and torsion. It is manifested by the underestimated fatigue lifes - the mean error parameter E_m is negative $E_m = -0.58$.

Table 4. Error life parameters for the analysed multiaxial fatigue failure criteria

	Matake	Findley, k				max$\{\sigma_n\}$	Max$\{\sigma_n, \tau_{ns}\}$
		0.0	0.2	0.4	0.8		
E_{std}	0.46	0.69	0.44	0.43	0.58	0.56	0.32
E_m	-1.14	0.05	-0.60	-1.38	-2.96	-0.40	-0.58

Conclusions

The following general conclusion appears: the critical plane and the fracture plane notions must be separated. The critical plane is simply a plane that used in the fatigue life assessment. The fracture plane at the microscale/macroscale is a plane where material cohesion is lost. Depending on loading levels, state of stress etc. the critical plane and fracture plane orientations may or not coincide. We postulate that the critical plane approach may be successfully used in the fatigue life estimation under different test conditions but the proposed damage parameter should be equivalent to the uniaxial one not only in term of the total fatigue life but also in term of the macroscopic fracture plane behaviour. For example, if under uniaxial torsion loading for a given fatigue life, some macroscopic cracks coincide with the maximum shear stress plane and other with the maximum normal stress plane than the fatigue criterion based on the torsion S-N curve should be used in the fatigue life estimation if the same fracture behaviour is revealed under multiaxial loading.

Although, plastic strains were taken into account, the computed fatigue lifes T_{cal} are underestimated (conservative). It means that the influence of stress gradient on the fatigue life cannot be neglected.

References
1. Findley, W.N. (1959), A theory for the effect of mean stress on fatigue of metals under combined torsion and axial load or bending, Journal of Engineering for Industry, November, 301-306.
2. Matake, T. (1977), An explanation on fatigue limit under combined stress, Bulletin of The Japan Society of Mech. Eng. **20**, 257-263.
3. Fatemi, A. and Socie, D.F. (1988), A critical plane approach to multiaxial fatigue damage including out-of-phase loading, Fatigue Fract Engng Mater Struct **11**, 149–165.
4. Karolczuk A., Macha E. (2005), A review of critical plane orientations in multiaxial fatigue failure criteria of metallic materials, Int J Fracture **134**, 267-304
5. Forsyth, P.J.E. (1961), A two-stage process of fatigue crack growth. Proceedings of the Symposium on Crack Propagation, Cranfield, England, 76-94.
6. Park, J., Nelson, D. (2000), Evaluation of an energy-based approach and critical plane approach for predicting constant amplitude multiaxial fatigue limit, Int. J. Fatigue **22**, 23-39.
7. Backstrom, M., Marquis, G. (2001), A review of multiaxial fatigue of weldments: experimental results, design code and critical plane approaches, Fatigue Fract Engng Mater Struct **24**, 279-291.
8. Serensen, S.V., Kogayev, V.P. & Shnejderovich, R.M. (1975), Permissible Loading and Strength Calculations of Machine Components, Third Edn., Mashinostroenie, Moskva (in Russian).
9. Karolczuk, A., Macha, E. (2005), Fatigue fracture planes and expected principal stress directions under biaxial variable amplitude loading, Fatigue and Fracture of Engineering Materials and Structures **28**, 99-106.
10. Chu, C.C. (1984) A three-dimensional model of anisotropic hardening in metals and its application to the analysis of sheet metal formability, J. Mech. Phys. Solids Vol. 32, No. 3, 197-212.
11. Karolczuk, A. (2006), Plastic strains and the macroscopic critical plane orientations under combined bending and torsion with constant and variable amplitudes, Engineering Fracture Mechanics, **73**, 1629–1652.